

Joint Theoretical Experimental Investigation of the Electron Spin Resonance Spectra of Nitroxyl Radicals: Application to Intermediates in *in Situ* Nitroxide Mediated Polymerization (*in Situ* NMP) of Vinyl Monomers

Natalia Zarycz,^{†,‡} Edith Botek,[†] Benoît Champagne,^{*,†} Valérie Sciannaméa,[§] Christine Jérôme,[§] and Christophe Detrembleur[§]

Laboratoire de Chimie Théorique Appliquée, Facultés Universitaires Notre-Dame de la Paix, rue de Bruxelles, 61, B-5000 Namur, Belgium, Departamento de Física, Universidad Nacional del Nordeste, 3400 Corrientes, Argentina, and Center for Education and Research on Macromolecules (CERM), University of Liège, Sart-Tilman, B6, B-4000 Liège, Belgium

Received: April 23, 2008; Revised Manuscript Received: May 29, 2008

Density functional theory (DFT) calculations have been performed to address the structure of nitroxide intermediates in controlled radical polymerization. In a preliminary step, the reliability of different theoretical methods has been substantiated by comparing calculated hyperfine coupling constants (HFCCs) to experimental data for a set of linear and cyclic alkyl nitroxyl radicals. Considering this tested approach, the nature of different nitroxides has been predicted or confirmed for (a) the reaction of *C*-phenyl-*N*-*tert*-butylnitron and AIBN, (b) *N*-*tert*-butyl- α -isopropylnitron and benzoyl peroxide, (c) *tert*-butyl methacrylate polymerization in the presence of sodium nitrite as mediator, and (d) for the reaction of a nitroso compound with AIBN. Values of HFCC experimentally determined have been confirmed by DFT calculations.

Introduction

Owing to its ability to be carried out under milder experimental conditions than ionic polymerization, nitroxide-mediated polymerization (NMP)^{1,2} is one of the most advantageous and promising techniques of controlled radical polymerization (CRP). Indeed, it allows controlling the molecular weight, the mass distribution, and the polymer architecture while it is metal-free and performs well for a wide variety of monomers. The control of the NMP process relies on the reversible capture of the propagating species by nitroxides to form dormant alkoxyamines. Different ways were developed to perform NMP. The two most usual routes consist (i) in initiating the polymerization of the vinyl monomer by a conventional free radical initiator in the presence of a nitroxide active in NMP,³ or (ii) in using an alkoxyamine having the dual role, i.e., initiating and controlling the polymerization, by thermal cleavage into the initiating radical and the nitroxide.⁴ Besides these conventional strategies, several researchers have contemplated the direct formation of nitroxides and alkoxyamines in the polymerization medium from readily and/or commercially available and inexpensive precursors.² Both the initiating radicals and the mediators (nitroxides) are produced in a one-pot technique, designated as *in situ* nitroxide-mediated polymerization (*in situ* NMP). A large variety of nitroxide precursors has been considered, which includes nitrones, nitroso compounds, hydroxylamines, secondary amines, sodium nitrite and nitric oxide.² However, the main drawback of this technique is that, because of the complexity of the reaction medium and different possible competing reactions, elucidation of the structure of the nitroxides *in situ* formed is not an easy task.

Electron spin resonance (ESR) spectroscopy has proved to be a useful technique for studying nitroxides⁵ and was imple-

mented in these *in situ* NMP processes. The physical background of ESR is analogous to this of the nuclear magnetic resonance (NMR) spectroscopy, though in the former the interactions of electromagnetic radiation are considered with the electron magnetic moments instead of the magnetic moments of the nuclei. As for NMR, ESR is employed *in vivo* and in several imaging applications.⁶

An efficient approach consists in coupling these experimental characterizations to theoretical modeling for addressing the reaction mechanisms^{7,8} as well as the structures⁹ and properties¹⁰ of polymeric materials. This is the approach adopted here to analyze experimental ESR spectra and to unravel the structures of the related compounds in the light of recent experimental work. The major theoretical aspects are summarized in section two. The third section assesses the performance of the different theoretical schemes when applied to small nitroxide derivatives for which experimental data are available. In section four, ESR characterizations of reaction intermediates in NMP of styrene are carried out and analyzed in light of theoretical simulations to determine and/or to confirm their structures. Conclusions are drawn in the last section.

Theoretical and Computational Aspects

The hyperfine coupling constant (HFCC) arises from the interaction of unpaired electrons with the magnetic moments of the nearby nuclei. This magnetic interaction, which does not depend on the applied (magnetic) field, splits each Zeeman electronic energy level into several sublevels leading to the resulting hyperfine splitting in the electronic paramagnetic resonance (ESR) spectra.⁵ These splittings provide detailed information about the zone where the spin density is distributed and therefore about the corresponding molecular structure.¹¹ In fact, the hyperfine interaction is the result of two contributions: the Fermi contact term, called the isotropic term, and the dipolar contribution, called the anisotropic term, though in fluid

[†] Facultés Universitaires Notre-Dame de la Paix.

[‡] Universidad Nacional del Nordeste.

[§] University of Liège.

solutions only the Fermi contact term prevails because the anisotropic term is averaged out to zero by the Brownian motion of molecules. The Fermi contact term describes the quantum interaction associated with the finite probability of finding an electron at a given nucleus and therefore it depends on the spin density at the corresponding nucleus.⁵

Accurate evaluation of the HFCCs is difficult due to the important role of electron correlation effects and the need to employ extended basis sets to describe properly the spin density at the nuclei.¹² In addition, HFCCs are sensitive to the surroundings (the nature of the solvent) and to the conformation whereas in several cases vibrational averaging is required. In this work, with the goal of addressing rather large systems, DFT was selected to determine and analyze the HFCCs of nitroxide derivatives ranging from small compounds to models of polymerization products. Therefore, in a first step, the reliability of the method, and of its approximations, is assessed by performing comparisons with experimental data and/or with high-level *ab initio* calculations. The latter are obtained employing the coupled-cluster scheme including all single and double excitations (CCSD). Like in our previous work,¹³ three hybrid exchange-correlation (XC) functionals were selected and combined with the EPR-II and EPR-III¹⁴ basis sets. Among these functionals, the B3LYP functional containing 20% of Hartree–Fock (HF) exchange, which has also been employed in recent investigations on radicals,¹⁵ and the PBE0 and BHandHLYP functionals, which include 25% and 50% of HF exchange, respectively, allowing us to address the impact of exact exchange on the HFCCs. In the last decades, DFT approaches succeeded in predicting and interpreting the ESR parameters of a broad range of organic molecules.¹⁶ To investigate the solvent effects, the polarizable continuum method using the integral equation formalism model (IEF-PCM)¹⁷ as implemented in GAUSSIAN03¹⁸ was employed.

The geometrical structures of the different stable conformers of the nitroxide radicals were determined at the DFT level using the B3LYP XC functional and the 6-311G* basis set. Often, there exist more than one stable conformer and their energies are within a few kcal/mol. Subsequently, an averaging procedure based on Maxwell–Boltzmann (M–B) distribution is performed to get the molecular properties. All the geometry optimizations and HFCC evaluations were performed using the GAUSSIAN03 program package.¹⁸ Actually, the isotropic hyperfine coupling constants (iHFCCs) are considered and they will be denoted HFCCs all over this work for the sake of simplicity.

Modeling HFCCs of Small Nitroxyl Compounds

Several types of nitroxide radicals have been tackled involving acyclic and cyclic derivatives. The acyclic species include the nitrogen oxide, dihydronitroxyl, methylnitroxyl, dimethylnitroxyl, diethylnitroxyl, di-*n*-propylnitroxyl, and di-*tert*-butylnitroxyl. The cyclic compounds studied are piperidinyl-1-oxyl, 2,2,6,6-tetramethylpiperidinyl-1-oxyl (TEMPO), 2,2,6,6-tetramethyl-4-oxopiperidinyl-1-oxyl (4-Oxo-TEMPO) and *N*-oxy-2-azaadamantane.

Acyclic Alkylnitroxyl Radicals. HFCCs of the acyclic alkylnitroxyl radicals calculated using the EPR-II and EPR-III basis sets are listed in Tables 1 and 2. Table 1 provides reference values obtained at the CCSD level whereas Table 2 gives DFT results determined using different exchange-correlation functionals. For equivalent H atoms the arithmetic average of the HFCCs is given while for compounds that present more than one stable conformer, the HFCCs of all the conformers as well as their Maxwell–Boltzmann averages are reported to get deeper

TABLE 1: HFCCs (in mT) of Acyclic Alkylnitroxyl Radicals Calculated at the CCSD Level with the EPR-II and EPR-III Basis Sets and in Comparison with Experiment^a

compounds	atoms	EPR-II	EPR-III	experiment
nitrogenoxide	N	0.862	0.766	1.06 (gaseous phase) ^b
dihydronitroxyl	N	1.002	0.923	1.19 (CH ₃ OH) ^c
	H(α)	−1.141	−1.104	−1.19 (CH ₃ OH) ^c
methylnitroxyl	N	1.315	1.247	1.38 (CH ₃ OH) ^c
	H(α)	−1.023	−1.001	−1.38 (CH ₃ OH) ^c
	H(β)	0.987	0.999	1.38 (CH ₃ OH) ^c
dimethylnitroxyl	N	1.610	1.551	1.68 (aqueous) ^d / 1.52 (CCl ₄) ^c
	H(β)	0.893	0.908	1.47 (aqueous) ^d / 1.23 (CCl ₄) ^c
diethylnitroxyl				
conf1	N	1.571		
57.4%	H(β)	0.993		
conf2	N	1.541		
31.2%	H(β)	0.685		
conf3	N	1.271		
11.4%	H(β)	0.640		
M–B average	N	1.528		1.67 (aqueous) ^d
	H(β)	0.857		1.12 (aqueous) ^d

^a The HFCCs of the three conformers of diethylnitroxyl are listed in italics together with their relative population within Maxwell–Boltzmann distribution ($T = 298.15$ K). ^b Reference 5. ^c Reference 19. ^d Reference 20.

insight into the structure–property relationships. For comparison, experimental data are also included.

At the reference *ab initio* level, enlarging the basis set implies a decrease of the N HFCC by 0.06 to 0.10 mT, which does not necessarily result in a better agreement with the measurements. For the H(β) HFCCs, going from EPR-II to EPR-III leads to an increase by 0.01 mT, whereas the H(α) HFCCs increase by 0.02–0.04 mT. For N atoms, the CCSD method is able to reproduce the variations of HFCCs with the number and size of the alkyl substituents. As discussed later, the situation is more complex for the H(β) because solvent effects are rather strong. In general, enlarging the basis set from EPR-II to EPR-III does not improve the correlation between theory and experiment.

At the DFT level for the B3LYP, PBE0, and BHandHLYP XC functionals, the basis set effects accompanying the transition from the EPR-II to the EPR-III basis set are smaller than at the reference CCSD level, at least, for the N and H(α) HFCCs. Moreover, in the case of the N atoms, the basis set effect goes in the opposite direction with respect to the CCSD results, with a HFCC increase smaller or equal to 0.04 mT. This yields a better agreement with experiment for the B3LYP and PBE0 XC functionals, whereas for the BHandHLYP functional, it implies in most cases a small overestimation of the experimental values. For the H(α) and H(β) atoms, enlarging the basis set results in variations of similar amplitudes (up to 0.03 mT) though of different signs.

Considering the EPR-III results, the variations of HFCCs within the B3LYP, PBE0, and BHandHLYP exchange–correlation functionals show that the larger the percentage of HF exchange, the larger the amplitude of the N and H(α) HFCCs but the smaller the H(β) HFCC amplitude. Note that in the case of N atoms, there might be exceptions to this observation for the B3LYP and PBE0 functionals, which only differ by 5% of HF exchange. Moreover, the amplitude of the HFCCs variations with the percentage of Hartree–Fock exchange is larger for the N than for the H atoms. In the case of the N and H(α), this means that, among these three exchange–correlation functionals,

TABLE 2: Theoretical versus Experimental HFCCs (in mT) of Acyclic Alkylnitroxyl Radicals^a

compounds	atoms	EPR-II			EPR-III			experiment
		B3LYP	PBE0	BHandHLYP	B3LYP	PBE0	BHandHLYP	
nitrogenoxide	N	0.607	0.535	1.066	0.647	0.548	1.079	1.06 (gaseous phase) ^b
dihydronitroxyl	N	0.866	0.858	1.119	0.885	0.858	1.126	1.19 (CH ₃ OH) ^c
	H(α)	−0.898	−0.923	−1.140	−0.900	−0.936	−1.148	−1.19 (CH ₃ OH) ^c
methylnitroxyl	N	1.122	1.131	1.418	1.149	1.141	1.438	1.38 (CH ₃ OH) ^c
	H(α)	−0.749	−0.784	−1.038	−0.767	−0.810	−1.058	−1.38 (CH ₃ OH) ^c
	H(β)	1.174	1.123	1.040	1.198	1.147	1.066	1.38 (CH ₃ OH) ^c
dimethylnitroxyl	N	1.361	1.391	1.706	1.387	1.402	1.730	1.68 (aqueous) ^d /1.52 (CCl ₄) ^c
	H(β)	1.044	1.003	0.949	1.061	1.023	0.972	1.47 (aqueous) ^d /1.23 (CCl ₄) ^c
diethylnitroxyl conf1 57.42%	N	1.314	1.344	1.678	1.330	1.345	1.688	
	H(β)	1.162	1.120	1.068	1.175	1.134	1.085	
conf2 31.21%	N	1.265	1.298	1.649	1.292	1.308	1.667	
	H(β)	0.799	0.770	0.741	0.817	0.787	0.759	
conf3 11.37%	N	0.946	0.990	1.401	0.979	1.005	1.419	
	H(β)	0.732	0.706	0.694	0.743	0.718	0.707	
M–B average	N	1.257	1.289	1.637	1.278	1.294	1.651	1.67 (aqueous) ^d
	H(β)	1.000	0.963	0.924	1.014	0.978	0.940	1.12 (aqueous) ^d
di- <i>tert</i> -butylnitroxyl conf1 25.03%	N	1.244	1.283	1.683	1.271	1.292	1.697	
conf2 25.02%	N	1.244	1.282	1.683	1.271	1.292	1.697	
conf3 24.98%	N	1.243	1.282	1.682	1.270	1.291	1.696	
conf4 24.97%	N	1.243	1.281	1.682	1.270	1.291	1.696	
M–B average	N	1.244	1.282	1.683	1.270	1.291	1.696	1.62 (diethyleneglycol) ^e /1.536 (C ₆ H ₆) ^f
di- <i>n</i> -propylnitroxyl conf1 21.32%	N	1.318	1.349	1.696	1.329	1.346	1.701	
	H(β)	1.243	1.196	1.143	1.256	1.211	1.159	
conf2 17.41%	N	1.288	1.318	1.663	1.303	1.318	1.672	
	H(β)	1.177	1.133	1.085	1.188	1.146	1.099	
conf3 14.51%	N	1.216	1.251	1.616	1.242	1.260	1.632	
	H(β)	0.833	0.802	0.774	0.852	0.821	0.793	
conf4 10.40%	N	1.291	1.319	1.656	1.310	1.323	1.669	
	H(β)	1.122	1.081	1.035	1.132	1.092	1.049	
conf5 9.55%	N	1.129	1.166	1.545	1.155	1.176	1.560	
	H(β)	0.816	0.786	0.763	0.831	0.802	0.778	
conf6 8.83%	N	1.202	1.236	1.597	1.231	1.248	1.615	
	H(β)	0.743	0.717	0.695	0.757	0.731	0.710	
conf7 6.08%	N	1.116	1.153	1.528	1.145	1.165	1.545	
	H(β)	0.744	0.718	0.700	0.755	0.730	0.712	
conf8 4.32%	N	0.938	0.982	1.393	0.970	0.995	1.409	
	H(β)	0.721	0.695	0.685	0.730	0.705	0.696	
conf. 9 3.02%	N	1.047	1.086	1.479	1.069	1.094	1.490	
	H(β)	1.000	0.966	0.943	1.014	0.981	0.957	
conf.10 2.56%	N	0.870	0.914	1.332	0.902	0.929	1.349	
	H(β)	0.814	0.787	0.777	0.824	0.799	0.789	
conf11 2.0%	N	1.213	1.250	1.619	1.234	1.256	1.631	
	H(β)	1.375	1.325	1.276	1.387	1.339	1.293	
M–B average	N	1.216	1.250	1.611	1.225	1.255	1.622	1.56 (ethanol) ^d
	H(β)	1.006	0.969	0.933	1.019	0.983	0.948	0.93 (ethanol) ^d

^a The calculations were performed using different exchange–correlation functionals with the EPR-II and EPR-III basis set. For compounds presenting several stable conformations, the HFCCs of the conformers and their relative weights within Maxwell–Boltzman distribution ($T = 298.15$ K) are listed together with the averaged values. ^b Reference 5. ^c Reference 19. ^d Reference 20. ^e Reference 21. ^f Reference 22.

the HFCC BHandHLYP values are the closest to the experimental values, whereas for the H(β) the values that are in better agreement with the measurements are those given by PBE0 and B3LYP functionals. Nevertheless, the three XC functionals are suitable to reproduce the variations in N and H(α) HFCCs with the chemical structure.

Several ESR studies on nitroxyl radicals have shown that the HFCCs are strongly solvent dependent.^{19–21} To investigate the solvent effects, the HFCCs were also calculated within the

IEFPCM scheme for toluene and methanol solutions as well as for water and CCl₄ in the case of the dimethylnitroxyl radical. These calculations, performed at the BHandHLYP/EPR-III level of approximation, employed the geometry that was optimized for the isolated species and are listed in Table 3. Accounting for the solvent effects within this polarizable continuum model—i.e., without considering explicitly the solvent molecules and their specific interactions with the solute—leads to a systematic increase on the N, H(α), and H(β) HFCC amplitudes,

TABLE 3: Solvent Effects on the HFCCs (in mT) Calculated at the BHandHLYP/EPR-III Level of Approximation within the IEFPCM Approach^a

compounds	atoms	in vacuo	in toluene	in methanol	experiment
nitroxide	N	1.079	1.080	1.081	1.06 (gas) ^b
dihydronitroxyl	N	1.126	1.206	1.306	1.19 (methanol) ^c
	H(α)	-1.148	-1.238	-1.347	-1.19 (methanol) ^c
methylnitroxyl	N	1.438	1.527	1.636	1.38 (methanol) ^c
	H(α)	-1.058	-1.135	-1.230	-1.38 (methanol) ^c
	H(β)	1.066	1.150	1.258	1.38 (methanol) ^c
dimethylnitroxyl	N	1.730	1.826	1.945	
			1.792 (CCl ₄)		1.52 (CCl ₄) ^c
			1.918 (water)		1.68 (water) ^d
	H(β)	0.972	1.042	1.133	
			1.011 (CCl ₄)		1.23 (CCl ₄) ^c
			1.140 (water)		1.47 (water) ^d
diethylnitroxyl	N	1.651	1.706	1.794	1.67 (water) ^d
	H(β)	0.940	0.922	0.953	1.12 (water) ^d
<i>n</i> -dipropylnitroxyl	N	1.622	1.670	1.796	1.56 (ethanol) ^d
	H(β)	0.948	0.899	0.957	0.93 (ethanol) ^d
di- <i>tert</i> -butylnitroxyl	N	1.696	1.750	1.826	1.62 (diethyleneglycol) ^e
					1.536 (benzene) ^f

^a For diethylnitroxyl, di-*n*-propylnitroxyl, and di-*tert*-butylnitroxyl only the M-B averages are listed. ^b Reference 5. ^c Reference 19. ^d Reference 20. ^e Reference 21. ^f Reference 22.

at least when considering the conformers individually. Indeed, in the case of diethylnitroxyl and di-*n*-propylnitroxyl in toluene, solvent effects strongly modify the M-B distribution so that the global solvent effect is a decrease of the H(β) HFCCs. Then, this increase is about twice as large for methanol than for toluene, demonstrating a saturation of the solvent effects with the dielectric constant ($\epsilon_{\text{toluene}} = 2.379$; $\epsilon_{\text{methanol}} = 32.63$) or a quasi linear evolution as a function of the $(\epsilon - 1)/(2\epsilon + 1)$ ratio. Note that this increase in HFCCs is consistent with a polarity-induced increase of the weight of the zwitterionic resonance form ($R_1R_2-N^{+}-O^{-}$) with respect to the form where the unpaired electron is located on the O atom ($R_1R_2-N-O^{\bullet}$). Considering the experimental data for protic solvents, it turns out that the IEFPCM(methanol)/BHandHLYP approach overestimates experiment, demonstrating that the good agreement between gas phase BHandHLYP data and experimental data in solution results partly from a compensation of errors between solvent effects and electron correlation treatment. Further analysis for the dimethylnitroxyl radical shows that the present solvation model can describe appropriately the solvent effects on the HFCCs. Then, though there might be quantitative improvements upon inclusion of solvent effects within the IEFPCM scheme, there is no dramatic change with respect to reproducing the trend in HFCCs as a function of the chemical structure.

Cyclic Alkylnitroxyl Radicals. Table 4 lists the HFCCs obtained with the three hybrid XC functionals and the EPR-III basis set for four cyclic alkylnitroxyl radicals: piperidinylnitroxyl, 2,2,6,6-tetramethylpiperidinylnitroxyl (TEMPO), 2,2,6,6-tetramethyl-4-oxopiperidinylnitroxyl (4-Oxo-TEMPO), and *N*-oxy-2-azaadamantane. Calculations show that piperidinylnitroxyl adopts a chair conformation as it happens in solution²⁶ and for an analogous cyclic nitroxide (2,2,6,6-tetramethylpiperidin-4-ol-nitroxyl) in the solid state.²⁷ The 2,2,6,6-tetramethylpiperidinylnitroxyl radical also adopts a chair conformation whereas, for 4-Oxo-TEMPO, two conformations are in equilibrium: a chair and a twisted boat conformations where, for the latter, the N atom presents a more planar, less pyramidal, geometry. The chair conformation presents a $\theta[C(\text{Me}_2)\text{NOC}(\text{Me}_2)]$ torsion angle of 157.7° whereas for the twisted boat conformation, it attains 180.0°. In our calculations,

the chair conformation is slightly more stable (1.2 kJ/mol) than the twisted boat conformation but the ordering is reverted when accounting for the solvent effects on the geometries optimized in vacuo ($\Delta E = 1.6$ kJ/mol). Finally, *N*-oxy-2-azaadamantane displays a rigid structure.

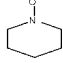
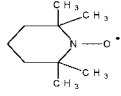
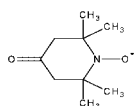
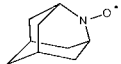
Like in the case of the acyclic compounds, for the four cyclic compounds, the N HFCCs increase with the amount of HF exchange and the best agreement with experiment is found when using the BHandHLYP functional. The effect of HF exchange on the H(β) atoms is smaller and the PBE0 functional yields usually the best quantitative agreement with experiment. The HFCCs of the H(γ) and H(δ) atoms are one order of magnitude smaller because these atoms are further distant from the radical center. In these cases, the effect of doubling the amount of HF exchange can be an increase by a factor of 2.

Because experimental data were available, Table 4 also reports some O and C HFCCs. For the O atoms, the B3LYP and PBE0 XC functionals underestimate the HFCC whereas the BHandHLYP functional overestimates it by a similar amount, foreseeing a better agreement with an intermediate (35–40%) of HF exchange. In the case of the C atoms, the behavior of their HFCCs with the amount of HF exchange follows the behavior of the H atoms attached to them. Indeed, for the C(α) and C(γ), the HFCCs increase but they decrease for the C(β). The best agreement with experiment is again obtained with the BHandHLYP functional.

Theory predicts larger N HFCCs for the chair conformation than for the twisted boat, reflecting the transition from a planar structure to a more pyramidal conformation of the bonds around the N atom as discussed in ref 23. Similarly, the pyramidal conformation of the N atom in the rigid *N*-oxy-2-azaadamantane structure leads to a further larger HFCC, close to 2 mT. Moreover, comparing piperidinylnitroxyl to 2,2,6,6-tetramethylpiperidinylnitroxyl, as well as to the chair conformation of 4-Oxo-TEMPO, reveals that the methyl groups on the C(α) modifies the spin density at the N site, yielding a decrease of HFCC by 0.04–0.09 mT.

Linear Regression Procedures. For the N HFCCs, linear regression fits were carried out; the fitted parameters are listed in Table 5 and Figure 1 provides a graphical comparison between the theoretical and experimental values. The fits are

TABLE 4: Theoretical versus Experimental HFCCs (in mT) of Cyclic Alkylnitroxyl Radicals

compounds	atoms	B3LYP	PBE0	BHandHLYP	experiment
<p>piperidinyl-1-oxyl</p> 	N	1.366	1.379	1.708	1.69 (CH ₂ Cl ₂) ^a
	H(β) _{ax}	2.084	2.019	1.929	2.015 (CH ₂ Cl ₂) ^a
	H(β) _{eq}	0.392	0.381	0.378	0.345 (CH ₂ Cl ₂) ^a
	H(δ)	-0.014	-0.020	-0.017	0.065 (CH ₂ Cl ₂) ^a
	(eq=ax)				
2,2,6,6-tetra-methyl-piperidinyl-1-oxyl (TEMPO)					
	N	1.277	1.294	1.680	1.615 (CH ₃ OH)/1.55 (toluene) ^b
	O	-1.464	-1.417	-2.490	-1.805 (CH ₃ OH)/-1.90 (toluene) ^b
	H(γ)	-0.038	-0.043	-0.046	-0.039 ^c
	H(γ')	-0.020	-0.027	-0.042	-0.023 ^c
	H(δ)	0.015	0.015	0.015	0.018 ^c
	C(α)	-0.298	-0.344	-0.474	-0.36 ^c
	C(β)	0.045	0.041	0.042	0.49 ^c
	C _{ax} (β')	0.582	0.572	0.549	0.49 ^c
	C _{eq} (β')	0.276	0.269	0.236	0.082 ^c
	C(γ)	-0.024	-0.027	-0.031	-0.032 ^c
2,2,6,6-tetra-methyl-4-oxopiperidinyl-1-oxyl (4-Oxo-TEMPO)					
<p>chair 62.1 %</p>	N	1.283	1.296	1.665	
	O	-1.471	-1.423	-2.510	
	H(γ)	-0.037	-0.043	-0.046	
	H(γ')	-0.013	-0.019	-0.035	
	C(α)	-0.320	-0.364	-0.482	
	C(β)	0.070	0.065	0.062	
	C(β')	0.409	0.403	0.372	
	C(γ)	-0.026	-0.030	-0.035	
	N	0.968	0.997	1.436	
	O	-1.470	-1.428	-2.522	
	H(γ)	0.006	0.000	-0.012	
	H(γ')	-0.004	-0.012	-0.028	
<p>Twisted boat 37.9 %</p>	N	0.968	0.997	1.436	
	O	-1.470	-1.428	-2.522	
	H(γ)	0.006	0.000	-0.012	
	H(γ')	-0.004	-0.012	-0.028	
	C(α)	-0.599	-0.648	-0.785	
	C(β)	0.219	0.216	0.206	
	C(β')	0.582	0.573	0.530	
	C(γ)	-0.025	-0.028	-0.031	
	N	1.163	1.183	1.578	1.445(C ₆ H ₆)/1.601(water) ^d
	O	-1.471	-1.425	-2.514	-1.929(C ₆ H ₆)/-1.786(water) ^d
	H(γ)	-0.021	-0.027	-0.034	-0.002 ^c
	H(γ')	-0.010	-0.017	-0.032	-0.012 ^c
<p>M-B</p> 	C(α)	-0.426	-0.472	-0.597	-0.51 ^c
	C(β)	0.126	0.122	0.117	0.23 (0.25) ^c
	C(β')	0.475	0.466	0.432	0.57 (0.61) ^c
	C(γ)	-0.025	-0.029	-0.033	-0.038 ^c
N-oxy-2-azaadamantane					
	N	1.674	1.681	1.989	1.975 (LiCl) ^e
	H(β)	0.210	0.205	0.202	0.295 (LiCl) ^e
	H(γ) _{eq}	-0.059	-0.066	-0.069	0.180 (LiCl) ^e
	H(γ) _{ax}	0.096	0.087	0.062	0.095 (LiCl) ^e
	H(δ)	0.060	0.055	0.044	0.19 (LiCl) ^e

^a Reference 26. ^b Reference 25. ^c Reference 23. ^d Reference 24. ^e Reference 28. ^f The calculations were performed using three XC functionals and the EPR-III basis set. For TEMPO, the HFCCs of the two stable conformers and their relative weight within Maxwell–Boltzmann distribution ($T = 298.15$ K) are listed together with the averaged values.

TABLE 5: Comparison between the Linear Regression Parameters Obtained between Calculated and Experimental N HFCCs of Nitroxide Compounds

method	basis set	<i>a</i>	<i>b</i>	<i>R</i> ²
HFCC(exp) = <i>a</i> × HFCC(theor) + <i>b</i>				
B3LYP	EPR-II	0.9182	0.4604	0.949
	EPR-III	0.9261	0.4277	0.952
PBE0	EPR-II	0.8345	0.5454	0.949
	EPR-III	0.8340	0.5388	0.951
BHandHLYP	EPR-II	0.9464	0.0757	0.974
	EPR-III	0.9364	0.0768	0.974
CCSD ^a	EPR-II	0.8498	0.3224	0.980
	EPR-III	0.7661	0.4682	0.994
BHandHLYP	EPR-III	0.7885	0.1947	0.930
IEFPCM (methanol)				

^a The CCSD/EPR-III fits were obtained using the data on nitrogen oxide, dihydronitroxyl, methylnitroxyl, and dimethylnitroxyl. In the case of CCSD/EPR-II, in addition to the above compounds, diethylnitroxyl is also considered.

of good quality as evidenced by the *R*² values larger than 0.93. The slope (*a*) and intercept (*b*) of the regressions are directly related to the performance of the level of approximation as well as to the completeness of the basis set. As observed for other properties,²⁹ these parameters are a function of the class of atoms and/or of the type of compounds, which explains why, for a given level of approximation, the *a* and *b* parameters of the nitroxides differ from those of radical cations of amino derivatives.¹³ Among the three hybrid XC functionals, the largest *R*² value is obtained for the BHandHLYP functional while the slope is the closest to unity and the intercept is the closest to zero. This numerically confirms the better quantitative performance of the BHandHLYP XC functional. Differences between the B3LYP and PBE0 functionals are small, though the B3LYP functional performs slightly better, contrary to the case of the N HFCCs in radical cations of amino derivatives. These differences between the functionals are further illustrated in Figure 2, which plots the PBE0 and BHandHLYP data as a function of the B3LYP N HFCCs. Figure 2 also shows that the B3LYP results are closer to the CCSD values than to the BHandHLYP ones. For all methods, the exp/theor slope is smaller than unity, which corresponds to a systematic overestimation by the theoretical schemes of the variations of N HFCCs with the chemical structure. These not only are due to the limitations of the level of approximation but also are related to compensation effects related to the lack of treatment of the solvent effects. Indeed, as presented in Table 3, linear regression for the IEFPCM(methanol)/BHandHLYP/EPR-III results does not lead to any improvement of the agreement with experiment. The linear regression parameters further demonstrate the similar quality of the EPR-II and EPR-III basis sets for describing nitroxide radicals. Though it performs similarly to the hybrid DFT approaches (Figure 2), it is difficult to comment more on the reliability of the CCSD method to provide quantitative agreement with experiment because the data set is rather limited. As a consequence, these linear regressions can be employed to improve the HFCC estimates. The root mean squares error (RMSE) between the B3LYP/EPR-III calculated and experimental values is equal to 0.34 mT. After the linear regression equation is applied to the calculated values, the RMSE decreases to 0.05 mT. Exactly the same behavior is observed for the PBE0 XC functional whereas for the BHandHLYP functional, these values attain 0.05 and 0.04 mT, i.e., showing

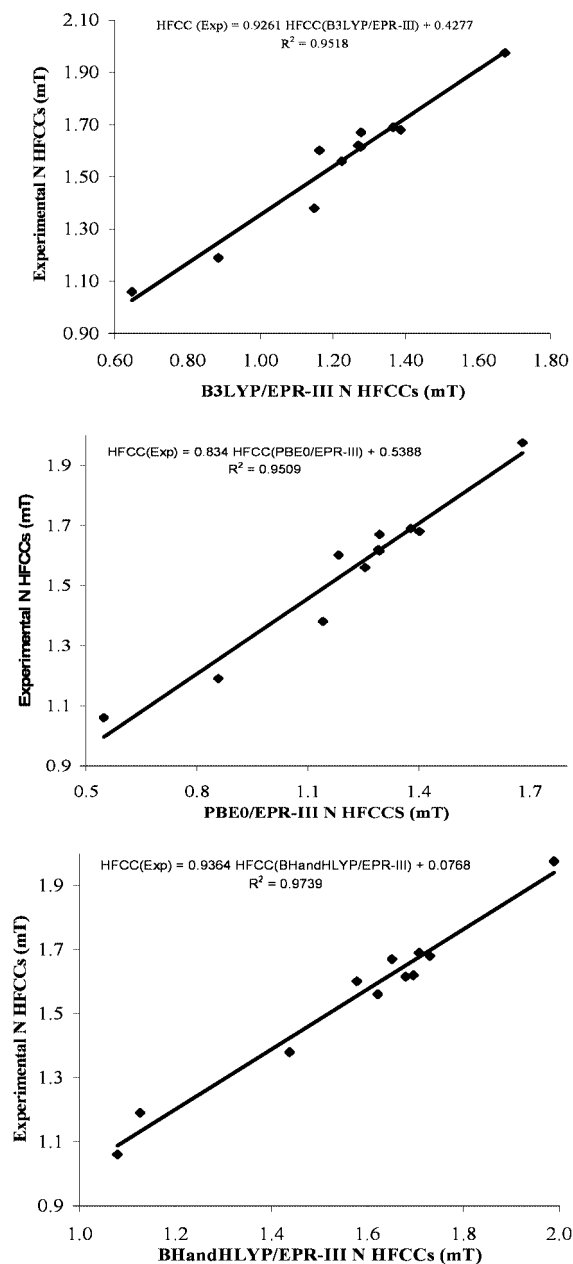


Figure 1. Relationship between the experimental HFCCs and the values evaluated at the B3LYP/EPR-III (top), PBE0/EPR-III (middle), and BHandHLYP/EPR-III (bottom) levels of approximation.

a very small improvement upon correcting the theoretical estimates, anyhow, the error being already small without linear fit correction. In summary, after correcting for the systematic deviations of the methods, there is no significant difference between the three hybrid XC functionals for predicting the HFCCs of N atoms in nitroxides and in the following, the broadly used B3LYP XC functional was employed.

HFCCs of Reaction Intermediates

Experimental studies have recently been performed with the aim of determining the structure of the formed nitroxides during some *in situ* NMP processes.

***In Situ* NMP of Styrene Mediated by the C-Phenyl-N-tert-butyl-nitron (PBN)/Azobis(isobutyronitrile) (AIBN) Pair.**^{30–32} The polymerization of styrene has been proved to be controlled by the PBN/AIBN pair, provided that the initiator (AIBN) and the

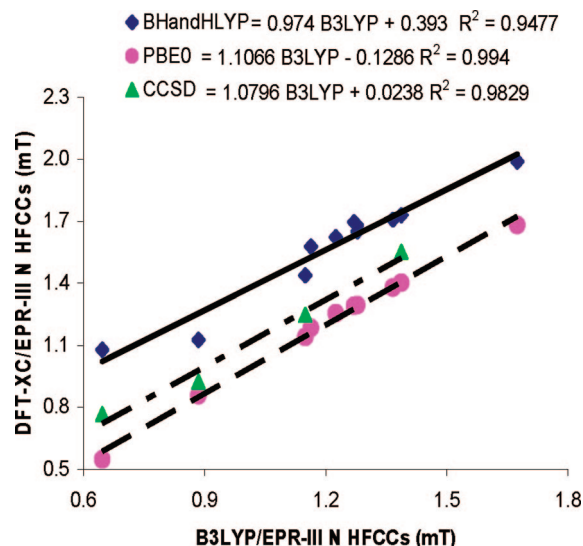
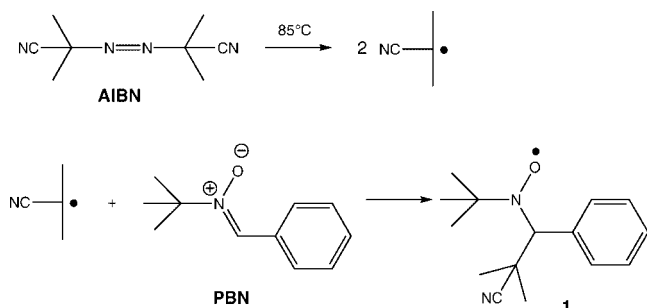


Figure 2. Relationship between the N HFCCs calculated using different methods of approximation in combination with the EPR-III basis set.

SCHEME 1: Nitroxide Formed When PBN and AIBN are Pre-reacted at 85 °C in Toluene without Styrene



precursor of nitroxides (PBN) are prereacted in toluene at 85 °C, prior to the addition of styrene and polymerization at 110 °C. Sciannamea et al.^{31,32} have concluded that the nitroxide formed during the prereaction results from the addition of an isocyanopropyl radical onto PBN according to Scheme 1. In toluene, this radical has HFCC values of 1.433 and 0.313 mT for the N and

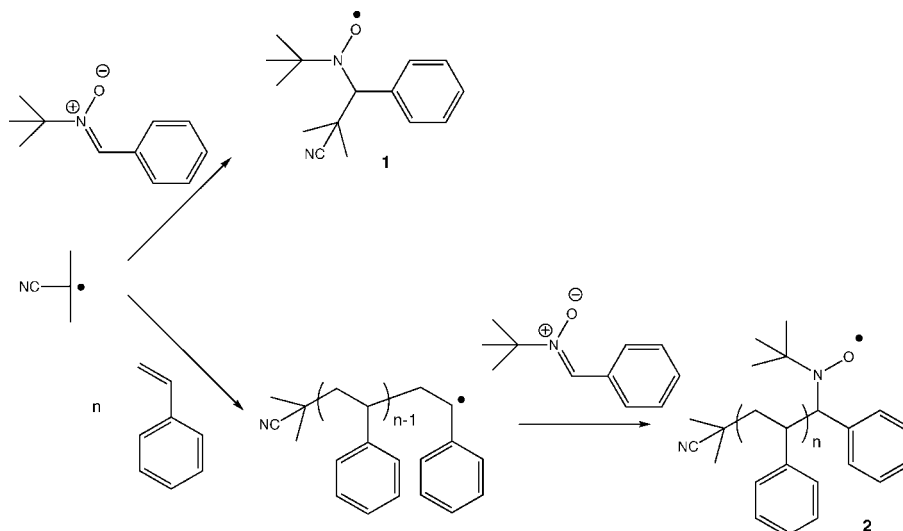
TABLE 6: Theoretical HFCCs Values (in mT) for Compounds 1 and 2 in Comparison with Experimental Data^a

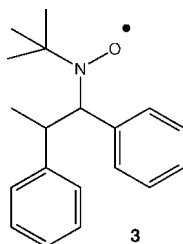
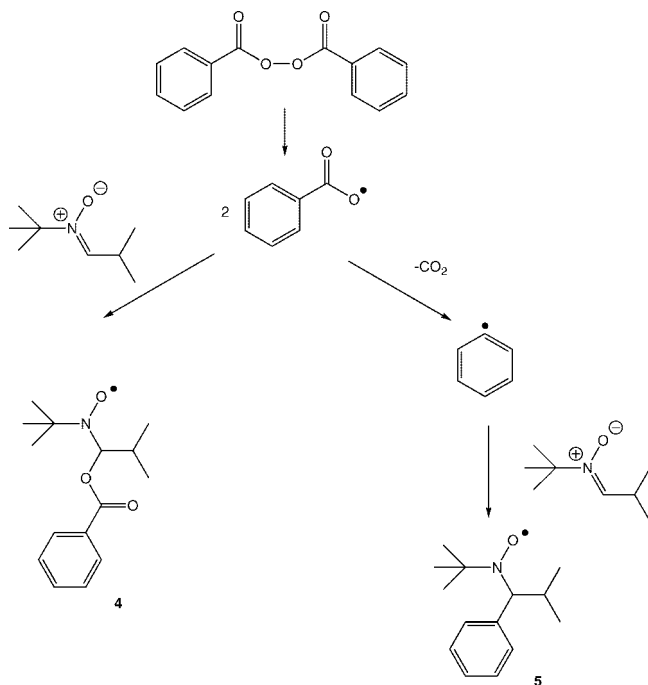
compound	atom	theory	experiment
1			
	conf1(53.5%)	N	1.477
		H(β)	0.257
	conf2(29.6%)	N	1.455
		H(β)	0.225
	conf3(16.9%)	N	1.434
M–B average			
	N	1.463	1.433 ^b
	H(β)	0.206	0.313 ^b
3	N	1.508	1.46 ^c
	H(β)	0.136	0.20–0.22 ^c

^a The theoretical values were obtained at the B3LYP/EPR-III level of approximation, and, for the N atoms, by employing the parameters of Table 5 for linear fit corrections. For **1**, the parameters are provided in italics for the different conformers as well as their M–B averages ($T = 298.15$ K). ^b In toluene with prereaction (see text for more details). ^c In toluene without prereaction.

H(β) atoms, respectively. On the other hand, when the PBN/AIBN/styrene mixture is directly heated at 110 °C without any prereaction step, two reaction pathways are possible.³² One implies the formation of compound **1**, the second one leads to the macronitroxide **2** by initiation of the styrene polymerization followed by trapping of the polystyryl macroradicals by PBN (Scheme 2). Again, the ESR signal is a sextuplet but the HFCCs are slightly different than in the other reaction conditions: for N and H(β), the HFCC values amount to 1.460 and 0.200 mT, respectively, and have therefore been attributed to the macronitroxide radical **2**. The nitroxide **3** (Scheme 3) has been used as a model of macronitroxide **2** for the DFT calculations. The theoretical DFT results listed in Table 6 support this assignment: the N HFCC values of **3** are larger than for **1** whereas the opposite behavior is observed for the H(β) atoms. In general, N HFCC as determined at this level of approximation, is slightly overestimated whereas H(β) HFCC is underestimated. Such remaining systematic differences with experiment are also observed in the next paragraphs. These calculations include the effects of the solvent (toluene) on the M–B distribution of the different conformers. Compound **1** can adopt three stable conformations, which differ by the torsion angle around the (H,N,O,Ph)C–C(Me,Me,CN) bond ($\theta = 60^\circ, 180^\circ, 300^\circ$) whereas

SCHEME 2: Nitroxides That May Be Formed When PBN and AIBN Are Heated at 110 °C in Toluene in the Presence of Styrene



SCHEME 3: Model Compound of Nitroxide 2 for DFT Calculation**SCHEME 4: Nitroxides Formed by Decomposition of BPO in the Presence of *N*-tert-Butyl- α -isopropyl nitron in Toluene at 85 °C**

there is only one stable conformer for **3** as a result of the presence of a bulky phenyl group on each C atom (Figure 3). A noticeable geometrical difference between **1** and **3** is the N–CH bond length, smaller for **1** (1.480 Å) than for **3** (1.486 Å). The O–N–C–H(β) torsion angle amounts to 162° and 165° for compounds **1** (conformer 1) and **3**, respectively.

In Situ NMP of Styrene Mediated by the *N*-tert-Butyl- α -isopropyl nitron/Benzoyl Peroxide (BPO) Pair in Toluene. The *N*-tert-butyl- α -isopropyl nitron/BPO pair was proved to impart control to the radical polymerization of styrene provided that a prereaction at 85 °C was carried out in the presence of

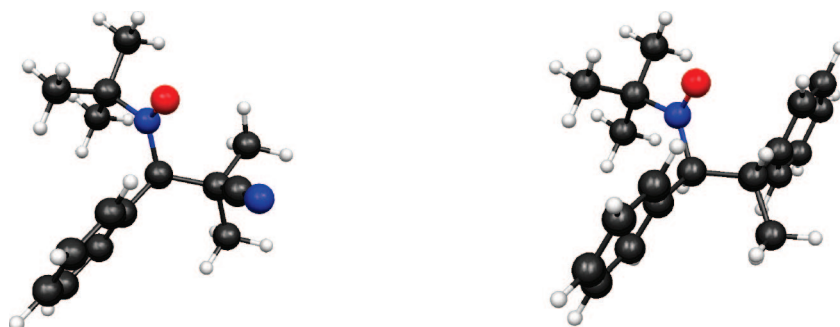
TABLE 7: B3LYP/EPR-III HFCCs Values (in mT, after Employing the Parameters of Table 5 for Linear Fit Corrections) for Compounds 4 and 5 in Comparison with Experimental Data^a

compound	atom	theory	experiment ^b
4	A (95.2%)	N	1.370
		H(β)	0.011
	B (2.0%)	N	1.370
		H(β)	0.146
	C (2.0%)	N	1.260
		H(β)	0.090
	D (0.8%)	N	1.366
		H(β)	0.175
M–B average	N	1.368	
	H(β)	0.017	
5	N	1.501	1.47
	H(β)	0.215	0.26

^a For **4**, the parameters are provided for the conformers (in italics) and for their M–B averages ($T = 298.15$ K). ^b In toluene.

styrene, prior to polymerization at 110 °C.³³ Because the monomer is present during this prereaction, few nitroxides may form during this prereaction, which makes this system quite difficult to characterize. To simplify the mechanism understanding, the *N*-tert-butyl- α -isopropyl nitron/BPO pair was prereacted in toluene at 85 °C prior to the addition of styrene and polymerization at 110 °C. Controlled polymerizations were also observed in these conditions.^{30,32} Depending on the decomposition pathway of BPO, nitroxides **4** and **5** may form during the prereaction (Scheme 4). The corresponding ESR spectrum is a sextuplet, characteristic of a nitroxide with a proton in β position. From the two proposed structures, compounds **4** and **5**, by comparison with other experimental data, it was established that the formed radical is TIPNO (compound **5**).³² It is characterized by a N HFCC of 1.47 mT and a H(β) HFCC of 0.26 mT (Table 7). The B3LYP/EPR-III approach provides HFCC values in close agreement with experiment (N, 1.501 mT; H(β), 0.215 mT): like for compounds **1** and **3**, N HFCC is slightly overestimated whereas H(β) HFCC is underestimated. Note that the N HFCC of compound **4** is quite smaller (1.368 mT) and cannot match the experimental data. The N HFCC of TIPNO is intermediate (1.501 mT) between those of compounds **1** (1.477 mT) and **3** (1.508 mT), which corresponds to a systematic HFCC increase with the C–N bond length (1.480, 1.483, and 1.486 Å for **1**, **4**, and **3**, respectively). Structures of **4** and **5** are sketched in Figure 4.

In Situ NMP of *tert*-Butyl Methacrylate in Water with Sodium Nitrite as Mediator.^{34–36} The controlled radical polymerization of *tert*-butyl methacrylate (tBMA) in water using sodium nitrite as mediator is another reaction for which the

**Figure 3.** Sketch of the geometrical structure of compounds **1** (conformer 1, left) and **3** (right).

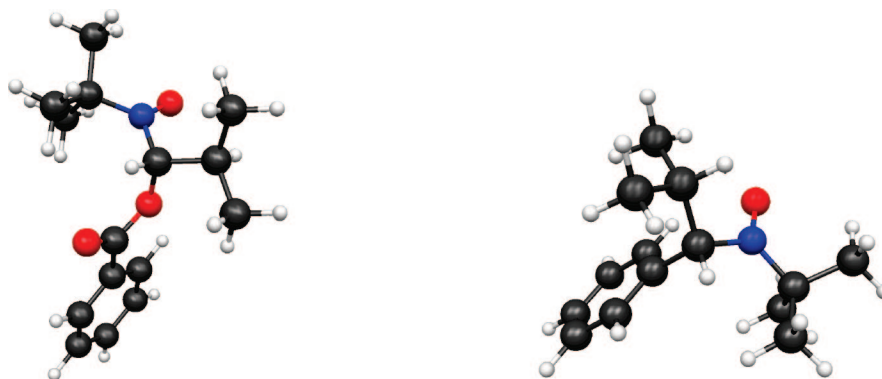
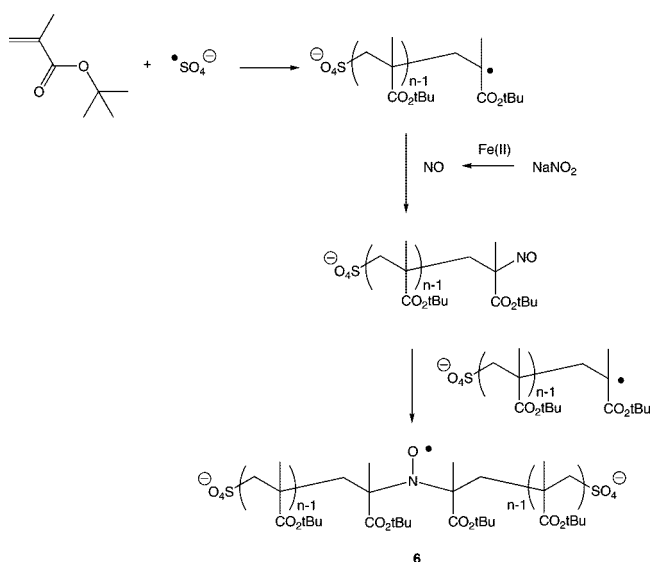
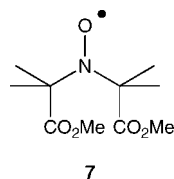


Figure 4. Sketch of the geometrical structure of compounds **4** (left) and **5** (conformer A, right).

SCHEME 5: Nitroxide Formed during the Polymerization of *tert*-Butyl Methacrylate Initiated by Potassium Persulfate in the Presence of Sodium Nitrite and Iron(II) Sulfate (or Ascorbic Acid)



SCHEME 6: Model Compound for the DFT Calculations of Nitroxide 6



postulated mechanism involves different nitroxides. Decomposition of sodium nitrite by iron(II) sulfate or ascorbic acid lead to nitric oxide which traps two propagating radicals to form the nitroxide **6** active in NMP (Scheme 5). This nitroxide was observed by ESR and presents a triplet with HFCC equal to 1.37 mT characteristic of a nitroxide bearing a nitrogen atom bonded to two tertiary carbons.^{34,35} To simplify the DFT calculations, nitroxide **7** (Scheme 6) was used as a reasonable model of nitroxide **6** by considering methyl formate groups in the place of *tert*-butyl formates and by replacing the polymeric chain by a methyl group. The theoretical values are presented in Table 8. DFT calculations predict very similar N HFCC values compared to the experimental value taking into account the preferential conformations determined by Maxwell–Boltzmann distributions. The three substituents on each quaternary C atom appear in staggered position with respect to each other

TABLE 8: Theoretical N HFCCs Values (in mT) for Compounds 7 and 9 in Comparison with Experimental Data^a

compound	theory	experiment ^b
7		
A (91.4%)	1.363	
B (0.4%)	1.414	
C (8.2%)	1.502	
M–B average	1.375	1.37
9		
A (63.9%)	1.389	
B (36.1%)	1.473	
M–B average	1.419	1.40

^a The theoretical values were obtained at the B3LYP/EPR-III level of approximation and by employing the parameters of Table 5 for linear fit corrections. The parameters are provided for the conformers (in italics) and for their M–B averages ($T = 298.15$ K).

^b From ref 34 in toluene.

providing the conformation is determined regarding along the axis defined by these two C atoms (Figure 5).

In Situ NMP of Methyl Methacrylate Mediated by Nitroso Compounds.³⁷ Nitroso compounds formed by reaction of nitric oxide (NO) and nitrogen dioxide (NO_2) with methyl methacrylate are also efficient nitroxides precursors active in NMP. The reaction of these nitroso compounds with AIBN produced rapidly nitroxides characterized by a triplet with a N HFCC value of 1.4 mT, characteristic of the nitroxide **8** (Scheme 7).³⁷ DFT calculations realized on the model compound **9** (Scheme 8) predict very similar coupling constant compared to the experimental data (Table 8). Once again, an average value of N HFCC has been determined by taking into account the preferential conformations of the nitroxide **9**.

Conclusions

Density functional theory calculations have been performed to address the structure of nitroxide intermediates in controlled radical polymerization. In a preliminary step, the reliability of different theoretical methods has been assessed by comparing calculated HFCCs to experimental data for a set of linear and cyclic alkyl nitroxyl radicals. For N HFCCs, the B3LYP, PBE0, and BHandHLYP exchange-correlation functionals provide nice linear relationships between the experimental and theoretical data, so that, after considering the linear fit corrections, the remaining root-mean-square error reduces to 0.05 mT. Moreover, for small nitroxides, these XC functionals predict N HFCC values in close agreement with the more elaborated CCSD calculations whereas considering solvent effects do not improve the quality of the linear relationships.

Considering this tested approach, the nature of different nitroxides has been predicted or confirmed for (a) the reaction

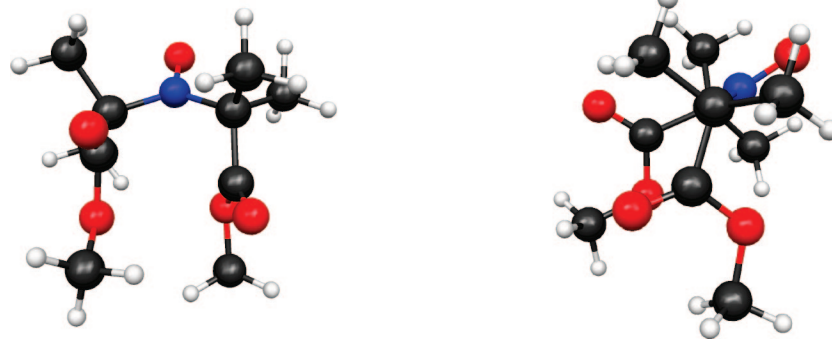
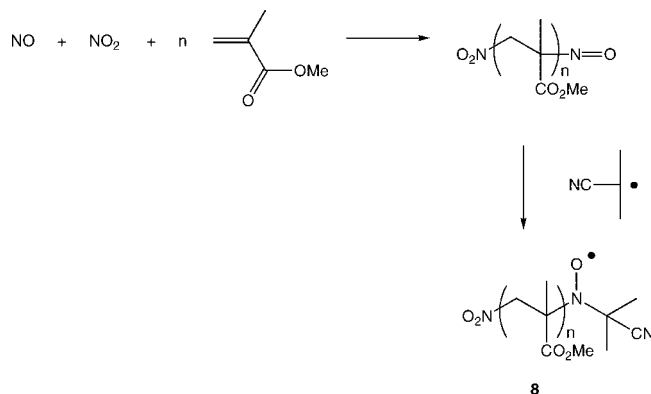
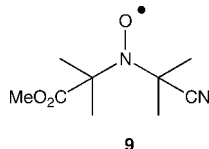


Figure 5. Sketch of the geometrical structures of compounds 7 (conformer A).

SCHEME 7: Nitroxide Obtained by Reaction of AIBN with the Nitroso Compound Formed by Reaction of NO and NO₂ with Methyl Methacrylate



SCHEME 8: Model Compound of Nitroxide 8



of C-phenyl-*N-tert*-butylnitron and AIBN, (b) *N-tert*-butyl- α -isopropylnitron and benzoyl peroxide, (c) *tert*-butyl methacrylate polymerization in the presence of sodium nitrite as mediator, and (d) for the reaction of a nitroso compound with AIBN. Values of HFCC experimentally determined have been confirmed by DFT calculations. N HFCC as determined at this level of approximation is, however, slightly overestimated compared to experimental values whereas H(β) HFCC is underestimated.

These results further demonstrate that this mixed theoretical/experimental approach can be applied to unravel the structures of radical intermediates in nitroxide-mediated polymerization reactions and therefore to discriminate between proposed reaction paths. Work along these lines are in progress in our laboratories.

Acknowledgment. This work was supported from research grants from the Belgian Federal Science Policy (IUAP No. P6-27 “Functional Supramolecular Systems”). N.Z. thanks the Consejo Nacional de Investigaciones Científicas y Técnicas (CONICET) for her Ph.D. grant. E.B. thanks the IUAP No. P6-27 for her postdoctoral grant. B.C. and C.D. thank the Fund for Scientific Research (FRS-FNRS) for their Research Director and Research Associate positions, respectively. The calculations have been performed on the Interuniversity Scientific Computing

Facility (ISCF), installed at the Facultés Universitaires Notre-Dame de la Paix (Namur, Belgium), for which we gratefully acknowledge the financial support of the FNRS-FRSC and the “Loterie Nationale” for the convention No. 2.4578.02, and of the FUNDP.

Supporting Information Available: Optimized geometries of the different conformers of compounds 1, 3, 4, 5, 7, and 9. The information is available free of charge via Internet at <http://pubs.acs.org>.

References and Notes

- (1) Hawker, C. J.; Bosman, A. W.; Harth, E. *Chem. Rev.* **2001**, *101*, 3661.
- (2) Sciannamea, V.; Jérôme, R.; Detrembleur, C. *Chem. Rev.* **2008**, *108*, 1104.
- (3) Georges, M. K.; Veregin, R. P. N.; Kazmaier, P. M.; Hamer, G. K. *Macromolecules* **1993**, *26*, 2987.
- (4) (a) Hawker, C. J.; Barclay, G. G.; Orellana, A.; Dao, J.; Devonport, W. *Macromolecules* **1996**, *29*, 5245. (b) Hawker, C. J. *J. Am. Chem. Soc.* **1994**, *116*, 11185. (c) Li, I. Q.; Howell, B. A.; Dineen, M. T.; Kastl, P. E.; Lyons, J. W.; Meunier, D. M.; Smith, P. B.; Priddy, D. B. *Macromolecules* **1997**, *30*, 5195. (d) Miura, Y.; Hirota, K.; Moto, H.; Yamada, B. *Macromolecules* **1998**, *31*, 4659.
- (5) Gerson, F.; Huber, W. *Electron Spin Resonance Spectroscopy of Organic Radicals*; Wiley-VCH: Germany, 2003.
- (6) Hirayama, A.; Nagase, S. *Nephron Clin Pract.* **2006**, *103*, 71.
- (7) (a) Coote, M. L.; Radom, L. *Macromolecules* **2004**, *37*, 590. (b) Coote, M. L.; Izgorodina, E. I.; Cavigliasso, G. E.; Roth, M.; Busch, M.; Barner-Kowollik, C. *Macromolecules* **2006**, *39*, 4585. (c) Chaffey-Millar, H.; Stenzel, M. H.; Davis, T. P.; Coote, M. L.; Barner-Kowollik, C. *Macromolecules* **2006**, *39*, 6406. (d) Van Cauter, K.; Van Den Bossche, B. J.; Van Speybroeck, V.; Waroquier, M. *Macromolecules* **2007**, *40*, 1321. (e) Lin, C. Y.; Coote, M. L.; Petit, A.; Richard, P.; Poli, R.; Matyjaszewski, K. *Macromolecules* **2007**, *40*, 5985. (f) Degirmenci, I.; Avci, D.; Aviyente, V.; Van Cauter, K.; Van Speybroeck, V.; Waroquier, M. *Macromolecules* **2007**, *40*, 9590.
- (8) (a) Champagne, B.; Mosley, D. H.; Fripiat, J. G.; André, J. M.; Bernard, A.; Bettonville, S.; François, Ph.; Momtaz, A. *J. Molec. Struct. (THEOCHEM)* **1998**, *454*, 149. (b) Monaco, G.; Toto, M.; Guerra, G.; Corradini, P.; Cavallo, L. *Macromolecules* **2000**, *33*, 8953. (c) Vyboishchikov, S. F.; Musaev, D. G.; Froese, R. D. J.; Morokuma, K. *Organometallics* **2001**, *20*, 309. (d) Khoroshun, D. V.; Musaev, D. G.; Vreven, T.; Morokuma, K. *Organometallics* **2001**, *20*, 2007. (e) Zurek, E.; Ziegler, T. *Organometallics* **2002**, *21*, 83. (f) Corradini, P.; Guerra, G.; Cavallo, L. *Acc. Chem. Res.* **2004**, *37*, 231. (g) Caporaso, L.; Gracia-Budria, J.; Cavallo, L. *J. Am. Chem. Soc.* **2006**, *128*, 16649. (h) Champagne, B.; Cavillot, V.; André, J. M.; François, Ph.; Momtaz, A. *Int. J. Quantum Chem.* **2006**, *106*, 588. (i) Stapleton, R. A.; Chai, J.; Nuanthanom, A.; Flisak, Z.; Nele, M.; Ziegler, T.; Rinaldi, P. L.; Soares, J. B. P.; Collins, S. *Macromolecules* **2007**, *40*, 2993. (j) Correa, A.; Piemontesi, F.; Morini, G.; Cavallo, L. *Macromolecules* **2007**, *40*, 9181. (k) Tomasi, S.; Razavi, A.; Ziegler, T. *Organometallics* **2007**, *26*, 2024.
- (9) (a) Meier, R. J.; van Doremale, G. H. J.; Iarlari, S.; Buda, F. *J. Am. Chem. Soc.* **1994**, *116*, 7274. (b) Koglin, E.; Meier, R. J. *Comput. Theor. Polym. Sci.* **1999**, *9*, 327. (c) Cavillot, V.; Champagne, B. *Chem. Phys. Lett.* **2002**, *354*, 449. (d) Lamparska, E.; Liégeois, V.; Quinet, O.; Champagne, B. *ChemPhysChem* **2006**, *7*, 2366. (e) d’Antuono, Ph.; Botek, E.; Champagne, B.; Wieme, J.; Reyniers, M. F.; Marin, G. B.; Adriaenssens, P. J.; Gelan, J. M. *Chem. Phys. Lett.* **2007**, *436*, 388.

- (10) (a) Soldera, A. *Polymer* **2002**, *43*, 4269. (b) Hu, W.; Mathot, V. B. F.; Frenkel, D. *Macromolecules* **2003**, *36*, 2165. (c) Sundararajan, P. R. *Polymer* **2004**, *45*, 1295. (d) Piel, C.; Karssenberg, F. G.; Kaminsky, W.; Mathot, V. B. F. *Macromolecules* **2005**, *38*, 6789. (e) Soldera, A.; Metatla, N. *Phys. Rev. E* **2006**, *74*, 061803.
- (11) Weil, J. A.; Bolton, J. R.; Wertz, J. E. *Electron Paramagnetic Resonance*; Wiley: New York, 1994.
- (12) (a) Sekino, H.; Bartlett, R. J. *J. Chem. Phys.* **1985**, *82*, 4225. (b) Feller, D.; Davidson, E. R. *J. Chem. Phys.* **1988**, *88*, 7580. (c) Furken, D.; Engels, B.; Peyerimhoff, S. D.; Grein, F. *Chem. Phys. Lett.* **1990**, *172*, 180. (d) Chipman, D. M. *Theor. Chim. Acta* **1992**, *82*, 93. (e) Feller, D.; Glendening, E.; McCullough, E. A., Jr.; Miller, R. J. *J. Chem. Phys.* **1993**, *99*, 2829. (f) Carmichael, I. J. *J. Phys. Chem.* **1995**, *99*, 6832. (g) Gauld, J. W.; Eriksson, L. A.; Radom, L. *J. Phys. Chem. A* **1997**, *101*, 1352. (h) Perera, S. A.; Salemi, L. M.; Bartlett, R. J. *J. Chem. Phys.* **1997**, *106*, 4061. (i) Mattar, S. M.; Stephens, A. D. *Chem. Phys. Lett.* **2000**, *327*, 409. (j) Al Derzi, A. R.; Fau, S.; Bartlett, R. J. *J. Phys. Chem. A* **2003**, *107*, 6656.
- (13) Rogowska, A.; Kuhl, S.; Schneider, R.; Walcarius, A.; Champagne, B. *Phys. Chem. Chem. Phys.* **2007**, *9*, 828.
- (14) Barone, V. I *Recent Advances in Density Functional Methods*; Chong, D. P., Ed.; World Scientific Publ. Co.: Singapore, 1995; Part I.
- (15) (a) Brown, E. C.; Borden, W. T. *J. Phys. Chem. A* **2002**, *106*, 2963. (b) Zhang, D. Y.; Hrovat, D. A.; Abe, M.; Borden, W. T. *J. Am. Chem. Soc.* **2003**, *125*, 12823. (c) Serwinski, P. R.; Esat, B.; Lahti, P. M.; Liao, Y.; Walton, R.; Lan, J. *J. Org. Chem.* **2004**, *69*, 5247. (d) Kubo, T.; Sakamoto, M.; Akabane, M.; Fujiwara, Y.; Yamamoto, K.; Akita, M.; Inoue, K.; Takui, T.; Nakatsuji, K. *Angew. Chem., Int. Ed.* **2004**, *43*, 6474. (e) Desmarests, C.; Champagne, B.; Walcarius, A.; Bellouard, C.; Omar-Amrani, R.; Ahajji, A.; Fort, Y.; Schneider, R. *J. Org. Chem.* **2006**, *71*, 1351. (f) Ali, Md. E.; Roy, A. S.; Datta, S. N. *J. Phys. Chem. A* **2007**, *111*, 5523.
- (16) (a) Wetmore, S. D.; Himo, F.; Boyd, R. J.; Eriksson, L. A. *J. Phys. Chem. B* **1998**, *102*, 7484. (b) Munzarova, M.; Kaupp, M. *J. Phys. Chem. A* **1999**, *103*, 9966. (c) Adamo, C.; Cossi, M.; Barone, V. *J. Molec. Struct. (THEOCHEM)* **1999**, *493*, 145. (d) Mattar, S. M.; Stephens, A. D. *Chem. Phys. Lett.* **2000**, *327*, 409. (e) Pauwels, E.; Van Speybroeck, V.; Lahorte, P.; Waroquier, M. *J. Phys. Chem. A* **2001**, *105*, 8794. (f) Engström, M.; Vaara, J.; Schimmelpfennig, B.; Ågren, H. *J. Phys. Chem. B* **2002**, *106*, 12354. (g) Truffier-Boutry, D.; Gallez, X. A.; Demoustier-Champagne, S.; Devaux, J.; Mestdagh, M.; Champagne, B.; Leloup, G. *J. Polym. Sci., Part A: Polym. Chem.* **2003**, *41*, 1691. (h) Pauwels, E.; Van Speybroeck, V.; Waroquier, M. *J. Phys. Chem. A* **2004**, *108*, 11321. (i) Rinkevicius, Z.; Telyatnyk, L.; Vahtras, O.; Ågren, H. *J. Chem. Phys.* **2004**, *121*, 7614. (j) Rohde, D.; Dunsch, L.; Tabet, A.; Hartmann, H.; Fabian, J. *J. Phys. Chem. B* **2006**, *110*, 8223. (k) Barone, V.; Polimento, A., *Phys. Chem. Chem. Phys.* **2006**, *8*, 4609. (l) Pauwels, E.; Van Speybroeck, V.; Waroquier, M. *J. Phys. Chem. A* **2006**, *110*, 6504.
- (17) (a) Cancès, E.; Mennucci, B.; Tomasi, J. *J. Chem. Phys.* **1997**, *107*, 3032. (b) Tomasi, J.; Cammi, R.; Mennucci, B.; Cappelli, C.; Corni, S. *Phys. Chem. Chem. Phys.* **2002**, *4*, 5697.
- (18) Frisch, M. J.; Trucks, G. W.; Schlegel, H. B.; Scuseria, G. E.; Robb, M. A.; Cheeseman, J. R.; Montgomery, J. A.; Vreven, T.; Kudin, K. N.; Burant, J. C.; Millam, J. M.; Iyengar, S. S.; Tomasi, J.; Barone, V.; Mennucci, B.; Cossi, M.; Scalmani, G.; Rega, N.; Petersson, G. A.; Nakatsuji, H.; Hada, M.; Ehara, M.; Toyota, K.; Fukuda, R.; Hasegawa, J.; Ishida, M.; Nakajima, T.; Honda, Y.; Kitao, O.; Nakai, H.; Klene, M.; Li, X.; Knox, J. E.; Hratchian, H. P.; Cross, J. B.; Bakken, V.; Adamo, C.; Jaramillo, J.; Gomperts, R.; Stratmann, R. E.; Yazyev, O.; Austin, A. J.; Cammi, R.; Pomelli, C.; Ochterski, J. W.; Ayala, P. Y.; Morokuma, K.; Voth, G. A.; Salvador, P.; Dannenberg, J. J.; Zakrzewski, V. G.; Dapprich, S.; Daniels, A. D.; Strain, M. C.; Farkas, O.; Malick, D. K.; Rabuck, A. D.; Raghavachari, K.; Foresman, J. B.; Ortiz, J. V.; Cui, Q.; Baboul, A. G.; Clifford, S.; Cioslowski, J.; Stefanov, B. B.; Liu, G.; Liashenko, A.; Piskorz, P.; Komaromi, I.; Martin, R. L.; Fox, D. J.; Keith, T.; Al-Laham, M. A.; Peng, C. Y.; Nanayakkara, A.; Challacombe, M.; Gill, P. M. W.; Johnson, B.; Chen, W.; Wong, M. W.; Gonzalez, C.; Pople, J. A. *Gaussian 03*, revision D.02; Gaussian, Inc.: Wallingford, CT, 2004.
- (19) Adams, J. Q.; Nicksic, S. W.; Thomas, J. R. *J. Chem. Phys.* **1966**, *45*, 654.
- (20) Hudson, A.; Hussein, H. A. *J. Chem. Soc. B* **1967**, 1299.
- (21) Lemaire, H.; Maréchal, Y.; Ramasseul, R.; Rassat, A. *Bull. Soc. Chim. Fr.* **1965**, 372.
- (22) Faber, R. J.; Markley, F. W.; Weil, J. A. *J. Chem. Phys.* **1967**, *46*, 1652.
- (23) Hatch, G. F.; Kreilick, R. W. *J. Chem. Phys.* **1972**, *57*, 3696.
- (24) Hayat, H.; Silver, B. L. *J. Phys. Chem.* **1973**, *77*, 72.
- (25) Aurich, H. J.; Hahn, K.; Stork, K.; Weiss, W. *Tetrahedron* **1977**, *33*, 969.
- (26) Rolfe, R. E.; Sales, K. D.; Utley, J. H. P. *J. Chem. Soc., Perkin Trans 2* **1973**, 1171.
- (27) Lajzerowicz-Bonneteau, J. *Acta Crystallogr.* **1968**, *B24*, 196.
- (28) Dupeyre, R. M.; Rassat, A. *Tetrahedron* **1978**, *34*, 1501.
- (29) (a) d'Antuono, Ph.; Botek, E.; Champagne, B.; Wieme, J.; Reyniers, M. F.; Marin, G. B.; Adriaenssens, P. J.; Gelan, J. M. *Chem. Phys. Lett.* **2005**, *411*, 207. (b) Champagne, B.; Guillaume, M.; Zutterman, F. *Chem. Phys. Lett.* **2006**, *425*, 105.
- (30) Sciannamea, V.; Guerrero-Sanchez, C.; Schubert, U. S.; Catala, J. M.; Jérôme, R.; Detrembleur, C. *Polymer* **2005**, *46*, 9632.
- (31) Sciannamea, V.; Catala, J.-M.; Jérôme, R.; Detrembleur, C. *J. Polym. Sci., Part A: Polym. Chem.* **2007**, *45*, 1219.
- (32) Sciannamea, V. Ph.D. Thesis, University of Liège: Liège, Belgium, 2006.
- (33) Detrembleur, C.; Sciannamea, V.; Koulic, C.; Claes, M.; Hoebeke, M.; Jérôme, R. *Macromolecules* **2002**, *35*, 7214.
- (34) Detrembleur, C.; Teyssié, P.; Jérôme, R. *Macromolecules* **2002**, *35*, 1611.
- (35) Detrembleur, C.; Mouithys-Mickalad, A.; Teyssié, P.; Jérôme, R. *e-Polymers*, online computer file; Paper No. 4; **2002**.
- (36) Vanhoorne, P.; Meyer, R.-V.; Detrembleur, C.; Jérôme, R. *Eur. Pat. Appl. EP 1236742*; Bayer A.-G.: Germany, 2002.
- (37) Detrembleur, C.; Claes, M.; Jérôme, R. *ACS Symp. Ser.* **2003**, *854*, 496.